ISSN 1027-4510, Journal of Surface Investigation: X-ray, Synchrotron and Neutron Techniques, 2018, Vol. 12, No. 3, pp. 436–441. © Pleiades Publishing, Ltd., 2018.

Study of the Microstructure, Crystallographic Structure and Thermal Stability of Al–Ti–Nb Alloys Produced by Selective Electron Beam Alloying[1]

S. Valkov[a], *, D. Neov[b], R. Bezdushnyi[c], A. Beskrovnyi[b], D. Kozlenko[b], and P. Petrov[a]

[a] *Institute of Electronics, Bulgarian Academy of Sciences, Sofia, 1784 Bulgaria*

[b] *Frank Laboratory of Neuron Physics, Joint Institute of Nuclear Research, Dubna, Moscow Region, Russia*

[c] *Department of Solid State Physics and Microelectronics, Faculty of Physics, Sofia University "St. Kliment Ohridski", Sofia, 1164 Bulgaria*

**e-mail: stsvalkov@gmail.com*

Received September 15, 2017

Abstract—This paper aims an investigation of the microstructure and crystallographic structure as well as the thermal stability of Al–Ti–Nb formed by selective electron beam surface alloying. The fabrication of the samples has been carried out using circular sweep mode, as two velocities of the sample movement have been chosen: V_1 = 1 cm/s and V_2 = 0.5 cm/s. The studied microstructure and crystallographic structure have been investigated by X-ray diffraction (XRD) and Scanning electron microscopy (SEM) respectively. The thermal behavior of the obtained surface alloys are evaluated by the coefficient of thermal expansion (CTE) which has been evaluated by neutron diffraction measurements at high temperature. The results show that in the earlier stages of formation, the microstructure of the intermetallic phase is mainly in the form of coarse fractions, but at the following moments they dissolve, forming separated alloyed zone and base Al substrate as the alloyed zone consists of fine $(Ti,Nb)Al_3$ particles dispersed in the Al matrix with small amount of undissolved intermetallic fractions. Formation of preferred crystallographic orientation as a function of the speed of specimen motion has not been observed. The performed neutron diffraction measurements show that the lattice parameters of the obtained intermetallic $(Ti,Nb)Al_3$ are less upshifted in comparison to pure Al. It has been found that the aluminium lattice is much more unstable at high temperatures than that of the intermetallic phase. The CTE for the intermetallic phase is 8.70 ppm/K for *a* axis and 7.75 ppm/K for *c* axis respectively while considering Al it is 12.95 ppm/K.

Keywords: selective electron beam alloying, X-ray diffraction (XRD), scanning electron microscopy (SEM), neutron diffraction, microstructure, crystallography, thermal behavior

DOI: 10.1134/S1027451018030187

1. INTRODUCTION

The development of new materials with attractive operational properties is of great interest for the modern industry. The evolution of some industrial branches is extremely important for improvement the quality of the human life. For that reason the production of light alloys with enhanced mechanical properties and high temperature performance is a target of the modern material science. These materials are widely used in the field of aerospace and aircraft manufacturing, automotive industry etc. [1–3].

Many studies concentrated on alloying of aluminium with different transition metals (e.g. Cu, Ti, Nb, etc.) have been conducted and the results demonstrate considerable improvement of the operational properties (e.g. microhardness, wear resistance, etc.) [4–7, 11]. A number of investigations exist describing the formation of the discussed materials by rapid solidification. This technique can be defined as an undercooling process where a preliminary deposited alloying element on aluminium substrate is treated by high intensity energy fluxes, such as electron and laser beams. This operation is able to form the so called "melt pool" and after the solidification of the melted zone the intermetallic material is obtained [8–10].

In study [7] a surface alloying of Al with Nb by laser beam is described and the results show a possibility to form Al_3Nb with body centered tetragonal DO_{22} structure – a hard intermetallic compound that melts at 1680°C. Another paper is focused on the formation of Al–Ti based materials by electron beam surface treatment and it is demonstrated a possibility to obtain Al_3Ti which melts at 1387°C [12].

[1] The article is published in the original.

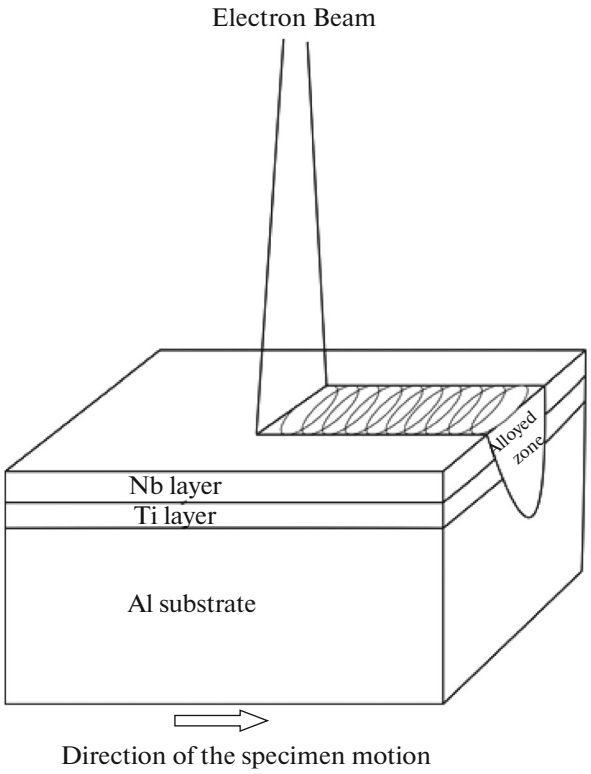

Fig. 1. Scheme of electron beam alloying technology.

Our previous results [13] demonstrate a selective electron beam technology of alloying of Al with Ti and Nb as a function of the applied technological conditions. It was observed a presence of a hard $(Ti,Nb)Al_3$ intermetallic phase (body centered tetragonal DO_{22} structure) formed in the soft α-Al matrix.

Since the performance of $(Ti,Nb)Al_3$ at high temperatures is of great importance for the modern industry its thermal behavior is a subject of discussion in this study as it is evaluated by the coefficient of thermal expansion.

This paper presents results of detailed investigation of the microstructure and crystallographic structure as well as the thermal stability of Al–Ti–Nb alloys formed by selective electron beam surface alloying.

2. EXPERIMENTAL PART

2.1. Sample preparation. The investigated Al–Ti–Nb surface alloys were produced as on commercially pure aluminium substrate, Ti and Nb coatings with thicknesses of about 2 μm were applied by DC (direct current) magnetron sputtering (MS). The diameter of the titanium and niobium targets was 100 mm with purity of 99.8 and 99.9% respectively. The process was realized in Ar medium as the working pressure was 1.2×10^{-1} Pa. The discharge voltage was 448 V, discharge current 1A and the deposition time was 2.5 hours for each coating. The obtained bilayer structure was then electron beam surface alloyed by scanning electron beam using circular mode. These technological conditions (i.e. circular mode) have been chosen due to the formation of homogenized structure of the obtained surface alloy as their influence on the homogenization process is extensively discussed in [13]. During the electron beam alloying process, the following technological parameters have been chosen: accelerating voltage 55 kV, electron beam scanning frequency 200 Hz, electron beam current 18 mA, focusing current 487 mA, and the diameter of the electron beam was 0.5 mm. The speed of the specimen motion was in the range from 5 to 0.5 cm/s and due to the high melting point of niobium low alloying speed is required. In order to investigate the influence of the speed of the specimen motion on the crystallographic structure and microstructure, two velocities have been chosen, namely $V_1 = 1$ cm/s and $V_2 = 0.5$ cm/s. Fig. 1 represents a scheme of electron beam alloying technology.

2.2. Samples characterization. The microstructure was investigated via Scanning Electron Microscopy (SEM/FIB LYRAI XMU, TESCAN), equipped with an EDX detector (Quantax 200,Bruker). In this study, back-scattered electrons were used with high voltage = 20 kV.

X-ray diffraction (XRD) methods were used to determine the crystallographic structure of the obtained samples. The measurements were performed on Seifert&Co diffractometer with CuK_α characteristic radiation. The patterns were registered in 2θ scale with step of 0.1° and counting time 10 s per step, as Bragg–Brentano (B–B) symmetrical mode has been applied.

The thermal stability of the obtained intermetallic compounds and adhesion to the substrate has been studied by evaluation of the coefficient of thermal expansion (CTE). For its determination neutron diffraction experiments at room temperature and 600 K were conducted. The measurements were carried out on DN-2 diffractometer of IBR-2 fast pulsed reactor located on the territory of Frank Laboratory of Neutron Physics (FLNP), Joint Institute for Nuclear Research (JINR), Dubna, Russia. It has been chosen backscattering ring detector for diffraction pattern acquisition due to the highest such among all detectors ($\Delta d/d < 0.01$). At the same time it covers wide range of d-spacings at middle d-values and has high efficiency around 50% (enabling gathering enough counting statistics for reasonably short period of time). The experiments have been conducted for 8 hours at room temperature and 600 K respectively.

3. RESULTS AND DISCUSSION

In Figs. 2a, 2b cross section SEM images of both samples are presented. The sample alloyed with V_1

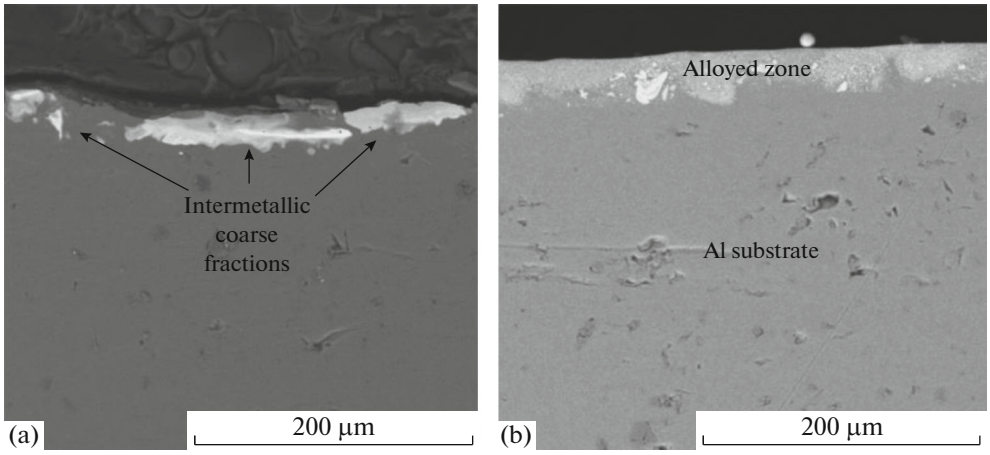

Fig. 2. Cross section SEM image of a sample alloyed with (a) V_1 and (b) V_2 velocity of movement of the samples.

speed of the specimen motion consists of intermetallic coarse fractions distributed in the α-Al matrix, while in the case of the treatment with V_2 velocity it consists of fine particles dispersed in α-Al with very small amount of intermetallic fractions in the alloyed zone. It is obvious that the microstructure strongly depends on the speed of the specimen motion during the alloying process. Low velocity corresponds to longer lifetime of the melt pool. In this case a clearly distinguished alloyed zone and base Al substrate are visible, which is contrary to the case of V_1 treatment (higher speed). Therefore, the microstructure evolution during the alloying process can be explained as a following: at the initial stages of the formation of surface alloys in the system of Al–Ti–Nb by means of selective electron beam treatment, the microstructure of the intermetallic phase is mainly in the form of coarse fractions distributed in the Al matrix. At the following moments of the alloying process, they dissolve forming a clearly distinguished alloyed zone, which consists of fine intermetallic particles dispersed in the Al matrix.

Figure 3 shows XRD patterns of the obtained samples alloyed with V_1 and V_2 respectively, registered in symmetrical Bragg-Brentano mode. Both patterns exhibit diffraction maximums, corresponding to intermetallic $(Ti,Nb)Al_3$ phase and pure Al, as all peaks are indexed. As it was mentioned above, $(Ti,Nb)Al_3$ is a pseudobinary compound, which is a solid solution between $TiAl_3$ and $NbAl_3$. Therefore, the identification of this phase was done according to both $TiAl_3$ (PDF# 37–1449) and $NbAl_3$ (PDF# 13–146) available at ICDD (International Center for Diffraction Data). It is visible that in both patterns, the strongest intermetallic peak is (112/103), which is in agreement with the data given at the crystallographic database. Table 1 summarizes the relative intensities of the diffraction maximums of the intermetallic compound experimentally obtained by XRD measurements and the values available at the ICDD database for $NbAl_3$ and $TiAl_3$.

The relative intensities of $NbAl_3$ and $TiAl_3$ peaks, published in ICDD are similar and the experimentally obtained results for both samples are in correlation with those applied in the crystallographic database. Therefore, the existence of strong crystallographic texture of the obtained surface coatings has not been observed. It should be noted that the peak corresponding to $2\theta = 65.13$ degrees in both patterns, shown in Fig. 2, is common for the pure Al and $(Ti,Nb)Al_3$. According to ICDD, the exact position of (220) Al, (204) $NbAl_3$ and (204) $TiAl_3$ is 65.133, 65.031, and 64.977 degrees at 2θ scale, respectively. Therefore, the influence of $(Ti,Nb)Al_3$ on the relative intensity of the discussed diffraction maximum is not enough clear. However, the discussed common peak is weaker than the maximum, corresponding to (112/103) crystallographic plane. These results are not in agreement with those published by R. Vilar et al. [14] where the crystallographic structure of Al_3Nb alloys formed by laser beam surface treatment has been studied. They have reported that strong (001) texture resulting from the solidification has been formed. Therefore, a significant difference between the texture formation of the laser and electron beam alloyed specimens has been observed. The laser processed surface alloys have dendritic microstructure, as the dendrites which have been predominantly growth at direction corresponding to the heat flow are privileged, which is able to form a strong texture. It should be mentioned that a significant difference between the microstructure of the electron and laser beam surface alloys has been observed [13, 15]. As it was already mentioned, the obtained microstructure of electron beam alloyed samples consists of intermetallic fractions randomly distributed in the Al matrix in the initial stages which is evolved to fine intermetallic particles dispersed in the base material with small amount of undissolved

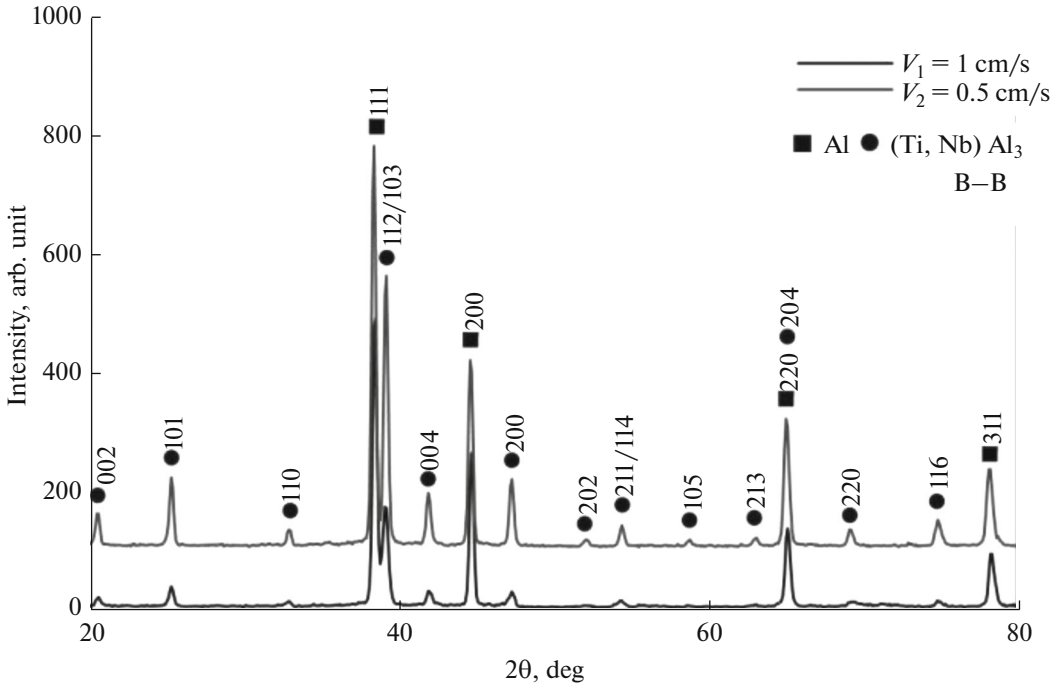

Fig. 3. Bragg–Brentano XRD patterns of electron beam surface alloyed samples at speed of the specimens motion V_1 = 1 cm/s and V_2 = 0.5 cm/s.

fractions in the alloyed zone, contrary to the case of laser beam alloyed specimens. Intermetallic dendrites were not observed and thus, the conditions of formation of strong textures were not realized in case of electron beam surface alloying. Many researchers have investigated the influence of the compositional and micro-structural parameters on the operational properties of the materials (i.e. microhardness, wear resistance etc.). According to authors [16, 17] the preferred crystallographic orientation can significantly affect them. At laser beam alloying, with increase of the scanning speed the microhardness also increases, while considering electron beam technology such effect has not been observed. This difference can be explained by the formation of strong (001) texture of laser alloyed samples.

The thermal behavior is evaluated by the coefficient of thermal expansion. It is important thermodynamic property of the crystalline materials describing the changes of the size of the linear coefficients and

Table 1. Relative intensities of XRD peaks

hkl	Relative intensities			
	V_1	V_2	ICDD PDF # 13-146 ($NbAl_3$)	ICDD PDF # 37-1449 ($TiAl_3$)
002	16.92	59.89	20	15
101	33.73	117.22	60	30
110	10.12	26.15	15	15
112/103	171.11	464.63	100	100
004	26.81	91.59	20	50
200	24.23	118.13	30	95
202	–	10.31	5	–
211/114	12.87	31.68	15	15
105	–	9.58	5	–
213	–	10.16	5	5
204	126.96	223.56	20	70
220	7.32	27.29	15	55
116	12.35	43.37	10	40

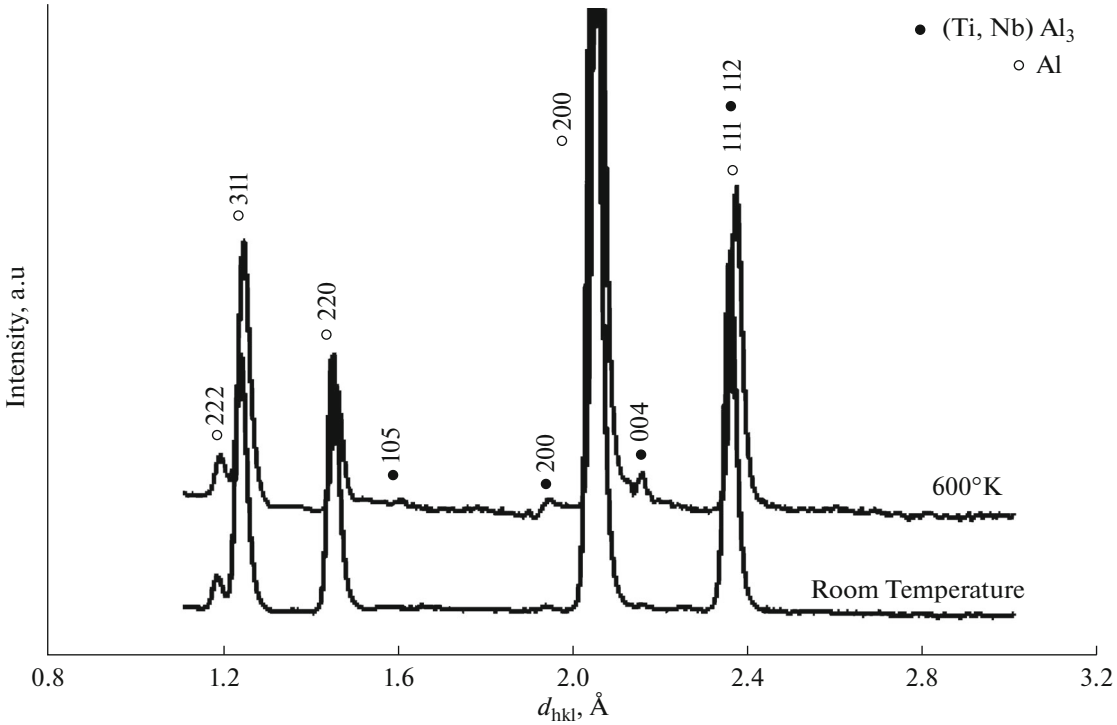

Fig. 4. Neutron diffraction pattern of Al–Ti–Nb alloy at different temperatures.

volume of the unit cell. The experimental CTE can be defined as a following:

$$(\mathrm{CTE})_a = \alpha_a = \frac{1}{a_0}\left(\frac{\partial a}{\partial T}\right), \quad (1)$$

$$(\mathrm{CTE})_c = \alpha_c = \frac{1}{c_0}\left(\frac{\partial c}{\partial T}\right), \quad (2)$$

$$(\mathrm{CTE})_V = \alpha_V = \frac{1}{V_0}\left(\frac{\partial V}{\partial T}\right), \quad (3)$$

Relations (2), (3), and (4) point to the coefficient of thermal expansion of *a*-axis, *c*-axis and cell volume respectively. In these formulas a_0, c_0 and V_0 are the initial values of *a* and *c* lattice parameters and the volume cell respectively. It should be noted that a neutron diffraction technique is significantly more appropriate method of evaluation the lattice parameters at high temperatures in comparison to the X-ray diffraction methods because of the deeper penetration depth of the neutrons. In this case the formed oxide phases on the surface of the investigated samples during the experiments at high temperature are not registered. The neutron diffraction pattern is shown in Fig. 4.

The pattern exhibits diffraction peaks of pure Al as well as maxima related to $(Ti,Nb)Al_3$. The experimentally evaluated lattice parameters of the intermetallic phase as well as of Al are shown in Table 2.

The CTE values obtained for the intermetallic compound and pure Al are shown in Table 3. It is obvious that CTE of the aluminium significantly exceeds that of the intermetallic phase which testifies of much more stable thermal behavior of $(Ti,Nb)Al_3$ in comparison to Al. In addition, the CTE of a axis is comparable with those of c one. This indicates that the bond strength of both axis is similar when considering the intermetallic compound and significantly higher in comparison to pure Al. Moreover, $(Ti,Nb)Al_3$ matrix role in strengthening of the material persists at elevated temperatures. Open question remains if the adhesion between Al and $(Ti,Nb)Al_3$ remains and how the different CTE of both contributes to rise of phase stresses during heating. This is very important for the

Table 2. Lattice parameters of $(Ti,Nb)Al_3$ and Al at room temperature and 600 K

Phase	a_{RT}, Å	c_{RT}, Å	$a_{600\ K}$, Å	$c_{600\ K}$, Å
$(Ti,Nb)Al_3$	3.83	8.60	3.84	8.62
Al	4.01	–	4.04	–

Table 3. Thermal expansion coefficient of $(Ti,Nb)Al_3$ and pure Al

Phase	CTE (*a*), ppm/K	CTE (*c*), ppm/K	CTE (*V*), ppm/K
$(Ti,Nb)Al_3$	8.70	7.75	27.74
Al	12.95	–	39.18

crack resistance and hence it could intimidate the structural integrity of the material at elevated temperatures, respectively after persistent heating/cooling cycles.

4. CONCLUSIONS

The results from this study demonstrate a possibility to form hard intermetallic surface coatings by electron beam surface alloying technique, which are applicable in the field of the high temperature performance.

The evolution of the microstructure and crystallographic structure and thermal behavior of $(Ti,Nb)Al_3$ formed by selective electron beam alloying are investigated. In the earlier stages of formation, the microstructure of the intermetallic phase is mainly in the form of coarse fractions, but at the following moments they dissolve, forming clearly separated alloyed zone and base Al substrate. The alloyed zone consists of fine $(Ti,Nb)Al_3$ particles dispersed in the Al matrix with small amount of undissolved intermetallic fractions as this phase composition has been confirmed by XRD experiments. The formation of preferred crystallographic orientation as a function of the speed of specimen motion during the alloying process has also been studied as the results show that the existence of strong texture has not been observed. The performed neutron diffraction measurements show that the lattice parameters of the obtained intermetallic $(Ti,Nb)Al_3$ are less upshifted in comparison to pure Al. It has been found that the aluminium lattice is much more unstable at high temperatures than that of the intermetallic phase. This statement was confirmed by the evaluation of the thermal expansion coefficients. The CTE for the intermetallic phase is 8.70 ppm/K for *a* axis and 7.75 ppm/K for *c* axis respectively while considering Al it is 12.95 ppm/K. The present results demonstrate that the pseudobinary $(Ti,Nb)Al_3$ intermetallic phase is characterized by improved mechanical properties, which are also retained at high temperatures, opening a number of novel practical applications.

5. ACKNOWLEDGMENTS

The authors are grateful to Dr. R. Lazarova for the preparation of the samples for cross section investigations. This work has been partially sponsored by the Bulgarian National Scientific Fund (Contract no. DN 07/16).

REFERENCES

1. H. Clements and S. Mayer, Adv. Eng. Mater. **15** (4), 191 (2013).
2. F. Appel, J. Paul and M. Oehring, *Gamma Titanium Aluminides: Science and Technology* (Wiley VCH, 2011).
3. D. Dimiduk, Mater. Sci. Eng., A **263** (2), 281 (1999).
4. A. Almeida and R. Vilar, Rev. Metal. (Madrid, Spain) **34** (2), 114 (1998).
5. W. Jiru, M. Sankar and U. Dixit, J. Mater. Eng. Perform. **25**, 1172 (2016).
6. U. Wendt, S. Settegast and I.-U. Grodrian, J. Matter. Sci. Lett. **22**, 1319 (2003).
7. A. Almeida, P. Petrov, I. Nogueira and R. Vilar, Mater. Sci. Eng., A **303**, 273 (2001).
8. L. Jacobson and J. McKittrick, Mater. Sci. Eng., R **11**, 355 (1994).
9. P. Petrov, Vacuum **48** (1), 49 (1997).
10. C. Draper and J. Poate, Int. Met. Rev. **30** (2), 85 (1985).
11. C. Reip and G. Sauthoff, Intermetallics **1**, 159 (1993).
12. P. Petrov, S. Valkov, R. Lazarova, S. Parshorov, R. Bezdushnyi, D. Dechev and N. Ivanov, J. Mater. Sci. Technol. (Sofia, Bulg.) **24** (2), 92 (2016).
13. S. Valkov, P. Petrov, R. Lazarova, R. Bezdushnyi and D. Dechev, Appl. Surf. Sci. **389**, 768 (2016).
14. R. Vilar, O. Conte and S. Franko, Intermetallics **7**, 1227 (1999).
15. S. Valkov, P. Petrov and R. Lazarova, Proc. SPIE **10226**, 102260I (2017). doi 10.1117/12.2262352
16. R. E. Reed-Hill and R. Abbachian, *Physical Metallurgy Principles* (PWS Publ., Boston, MA, 1994).
17. D. R. Ackerland, *The Science and Engineering of Materials* (PWS Engineering, Boston, MA, 1985).